Dentomaxillofacial Radiology (2017) 46, 20160355

birpublications.org/dmfr

RESEARCH ARTICLE

Clinical evaluation of the iterative metal artefact reduction algorithm for post-operative CT examination after maxillofacial surgery

[1]Arsany Hakim, [1]Johannes Slotboom, [2]Olivier Lieger, [2]Fabian Schlittler, [3]Roland Giger, [4]Chantal Michel, [1]Roland Wiest and [1]Franca Wagner

[1]Institute of Diagnostic and Interventional Neuroradiology, Bern University Hospital, Inselspital University of Bern, Bern, Switzerland; [2]Department of Craniomaxillofacial Surgery, Bern University Hospital, Inselspital University of Bern, Bern, Switzerland; [3]Department of Otorhinolaryngology—Head and Neck Surgery, Bern University Hospital, Inselspital University of Bern, Bern, Switzerland; [4]University Hospital of Child and Adolescent Psychiatry and Psychotherapy, Bern University Hospital, University of Bern, Bern, Switzerland

Objectives: Metal artefacts present challenges to both radiologists and clinicians during post-operative imaging. Such artefacts reduce the diagnostic effectiveness of CT scans and mask findings that could be vital for patient management. Thus, a powerful artefact reduction tool is necessary when imaging patients with metal implants. Our aim was to test the recently introduced iterative metal artefact reduction (iMAR) algorithm in patients with maxillofacial implants.
Methods: Images from 17 patients with diverse maxillofacial metal implants who had undergone CT scans were qualitatively and quantitatively analyzed before and after metal artefact reduction with iMAR.
Results: After iMAR application, images exhibited decreased artefacts and improved image quality, leading to detection of lesions that were previously masked by artefacts. The application of iMAR did not affect image quality in regions distant from the metal implants.
Conclusions: The application of iMAR to CT examinations of patients with maxillofacial metal implants leads to artefact reduction, improvement of image quality and increased diagnostic utility. Routine implementation of iMAR during imaging of patients with metal hardware implants could add diagnostic value to their CT examinations.
Dentomaxillofacial Radiology (2017) **46**, 20160355. doi: 10.1259/dmfr.20160355

Cite this article as: Hakim A, Slotboom J, Lieger O, Schlittler F, Giger R, Michel C, et al. Clinical evaluation of the iterative metal artefact reduction algorithm for post-operative CT examination after maxillofacial surgery. *Dentomaxillofac Radiol* 2017; **46**: 20160355.

Keywords: artefacts; CT; post-operative; metal; osteosynthesis; dental

Introduction

Metal hardware, such as prostheses, wires, pins, reconstruction plates and screws, are routinely used in maxillofacial surgery and patients who undergo such surgery commonly require post-operative imaging for follow-up or may undergo imaging for the investigation of other unrelated conditions. However, the presence of metal during a CT scan causes beam hardening, streaking, non-linear partial volume effects, noise, scatter and aliasing, which are collectively known as metal artefacts.[1,2] These artefacts significantly degrade image quality, restrict the evaluation of operative reconstruction and may mask post-operative pathologies, such as haemorrhage, infections or other incidental pathologies in nearby or distant regions (for example, tumours). Failure to note such findings may lead to serious complications and may impair patient management.

Correspondence to: Mr Arsany Hakim. E-mail: arsany_hakim@yahoo.com
Received 31 August 2016; revised 15 October 2016; accepted 11 January 2017

Some metal artefacts can be reduced by changing the scan parameters (such as milliampere second, kilovoltage or slice thickness) or by using a dedicated kernel and adding filters; however, the results of these modifications are not satisfactory.[1] Other new methods, such as dual-source scanners, require specialized equipment and reduce only some types of artefacts.[1,3]

For these reasons, CT vendors have been trying to implement new algorithms to reduce these artefacts. The modern algorithms for metal artefact reduction may differ between manufacturers but utilize the same principle, which is iterative reconstruction. In addition, many of these algorithms use "sinogram in-painting", which considers CT values affected by metal to be completely useless and ignores them. This deletion leads to loss of data in regions near the metal, or generates new artefacts. Owing to these drawbacks, other interpolation techniques are used to replace the corrupted data.[4,5] The iterative metal artefact reduction (iMAR) algorithm was recently introduced by Siemens Healthcare and is based on two previously developed algorithms, namely frequency split metal artefact reduction (FSMAR) and normalized metal artefact reduction (NMAR).[6–8] NMAR minimizes new artefacts generated in the corrected image during interpolation by removing the structures with high contrast from the sinogram prior to the interpolation process and reinserting them afterwards.[4,6] FSMAR preserves both the natural image impression and the valid edge information of the uncorrected image, which has the drawback of reinserting high-frequency streak artefacts into the corrected image. These artefacts are reduced following each iteration so that the final image quality depends on the number of iterations. Other factors affecting image quality include the threshold used for metal segmentation and prior image calculation, as well as the filter parameters of the frequency split operation. These parameters are user selectable and vendor adjusted according to the metal implant type (for example: neuro, dental, prosthesis or pacemaker).[6,9] The process of iMAR has been discussed in detail by Axente et al[6] and Wuest et al.[9]

Previous studies on iMAR and its prototypes revealed its utility in reducing streak artefacts.[10–13] However, there are concerns that these newly introduced algorithms may not provide accurate attenuation values near metallic hardware and that this may impair diagnostic values by smoothing the image in attempts to reduce noise. This study was designed to address these concerns and to evaluate the performance of iMAR in patients with maxillofacial implants after reconstructive surgery or metallic implants, such as fixed overdentures.

Methods and materials

This retrospective study was conducted according to the guidelines of the Cantonal Ethics Committee and was performed in accordance with the guidelines of the Declaration of Helsinki. All CT examinations were clinically indicated, and no CT scan was performed for the purpose of this study alone.

Study population

A total of 17 (12 male and 5 female) patients who underwent CT for diverse indications at the Institute of Diagnostic and Interventional Neuroradiology, Inselspital, Bern University Hospital and University of Bern, Bern, Switzerland, were retrospectively analyzed. The inclusion criterion was the presence of metal hardware in the maxillofacial region. The age of the patients ranged from 19 to 89 years (mean 63 years).

Metal hardware

The 17 patients had diverse types of metal hardware. In 14 (82.4%) patients, multiple metal implants in different locations were present. Among our patient sample, approximately 32 metallic hardware implants (ranging from 2 cm × 0.5 cm to 9 cm × 1 cm in diameter) were examined, in addition to amalgam tooth fillings and dental superstructures.

Among the 17 patients, 13 (76.5%) patients had metal hardware in the maxilla and 11 (64.7%) patients had metal hardware in the mandible. 2 (11.8%) patients presented with maxillary internal fixation (plate and screws) and 8 (47.1%) patients presented with mandibular internal fixation. Most of the patients (70.58%) had multiple amalgam tooth fillings and/or dental pins. 1 (5.9%) patient also presented with bilateral orbital mesh implants. Figure 1 illustrates examples of the types of metal hardware analyzed in our study. Our patients had diverse types of metal ranging from silver amalgam, gold–platinum or silver–palladium to titanium.

Clinical indication

For 5 (29.4%) of the 17 patients, the indication for CT was a suspected infection in the oral cavity or mandible. 4 (80%) of these 5 patients presented to our emergency department with pain, soft-tissue swelling and limited mouth opening. The fifth patient presented with clinical signs of an infection after receiving a tongue piercing. 4 (23.5%) of the 17 patients in the study were under bisphosphonate therapy. These patients complained of pain when moving the mouth and when speaking, and CT scanning was performed to exclude osteonecrosis and pathological fracture of the mandible. 3 (17.6%) of the 17 patients were referred for a routine post-operative CT scan of the facial bones following severe trauma and complex maxillofacial reconstruction. For 2 (11.8%) patients, a muscle free flap transfer after tumour excision (of the head and neck) was planned, and a CT scan of the extracranial vessels was performed for pre-operative delineation of the vascular supply. For 2 (11.8%) patients, stroke work-up (CT brain scan and CT angiography) was performed in response to neurological symptoms. The last patient (5.9%) complained of recurrent nasal polyps and was referred for a CT scan for pre-operative planning.

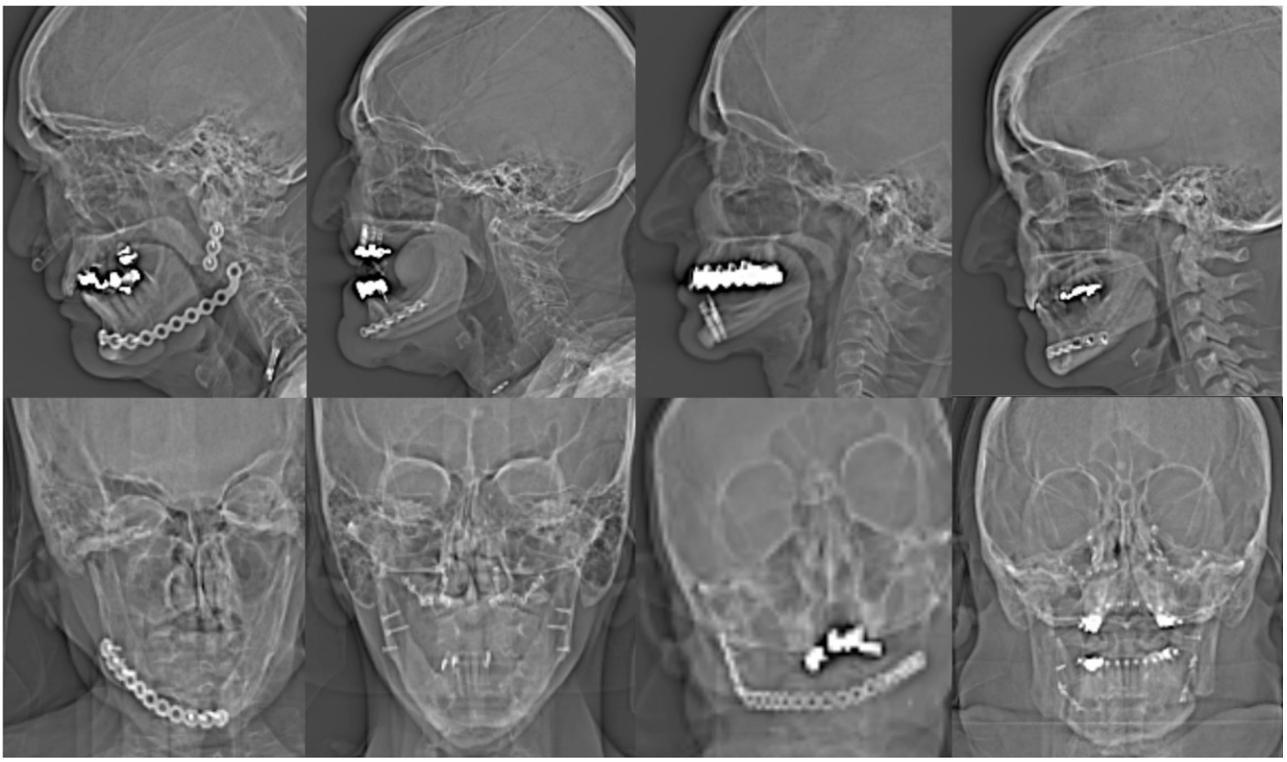

Figure 1 An example of metal hardware: CT topograms from eight patients with diverse implants ranging from plates with screws, dental fillings and dental pins to eye mesh.

CT image acquisition

All examinations were performed in the supine position using a 128-slice CT scanner (SOMATOM® Definition Edge; Siemens Healthcare, Erlangen, Germany). 6 (35%) patients underwent non-enhanced CT; 9 (53%) patients underwent contrast-enhanced CT of the facial bones; and 2 (12%) patients underwent non-enhanced CT/contrast-enhanced CT of the brain and CT angiography of the intracranial and extracranial vessels.

Image reconstruction according to our protocol includes a soft-tissue window (kernel J45s) and a bone window (kernel J70h). Both images are routinely reconstructed using the standard integrated sinogram-affirmed iterative reconstruction (SAFIRE) algorithm.

Iterative metal artefact reduction (artefact reduction algorithm)

For the purpose of our study, the soft-tissue window was reconstructed using the iMAR algorithm. iMAR was developed by Siemens Healthcare based on the previous algorithms FSMAR and NMAR. The iMAR process has been discussed in detail by Axente et al[6] and Wuest et al.[9] iMAR is an add-on tool to the scanning software that is implemented similarly to the standard SAFIRE algorithm without any need for operator training. Additional reconstruction with iMAR takes from a few seconds to a few minutes (according to the number of images to be reconstructed) and does not delay other reconstructions of the standard images being transferred to the picture archiving and communication system. Post-processing with iMAR can be performed even after the examination is finished as long as the source images remain in the scanning computer.

The images before post-processing are referred to as the uncorrected data set. The iMAR images after post-processing are referred to as the corrected data set.

Image evaluation and measurements

A certified reporting workstation (Sectra IDS7, Linköping, Sweden) with a certified monitor (DIN V 6868-57 and QA guideline) was used for the analysis. The evaluation of both data sets, *i.e.* uncorrected and corrected with iMAR, was performed independently by two experienced neuroradiologists (AH and FW). Window settings could be adjusted by the examiners. The axial soft-tissue reconstruction kernel was utilized with the soft tissue and bone windows. To avoid a partial volume effect, all analyses were performed on thin slices (0.6–1 mm).

Qualitative image analysis

Three criteria (artefacts, image quality and diagnostic utility) were defined. The first two criteria were assessed on a four-point scale in six defined regions of the image (three on each side, R1 to R3 and L1 to L3 at the level of the oropharynx) (Figure 2). The six defined regions were symmetrically separated with a vertical line from the symphysis menti to the centre of the tip of the dens

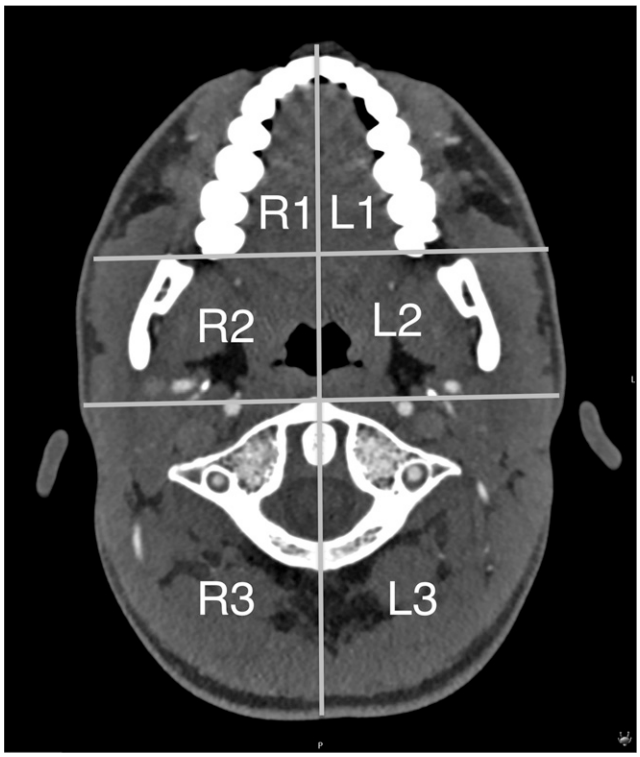

Figure 2 The six defined regions for artefact and image quality analysis.

axis and the middle of the posterior cervical arch. A horizontal line connected both posterior maxillary ridges, and a second line was placed immediately ventral to the atlas.

These lines separated three regions on each side into the anterior, middle and posterior regions. The anterior regions (R1 and L1) included the oral cavity and submandibular spaces. The middle regions (R2 and L2) included the parapharyngeal spaces, masticator spaces and pharyngeal mucosal spaces. The posterior regions (R3 and L3) included the perivertebral spaces and posterior cervical spaces.

Artefacts

The severity of artefacts was evaluated using a four-point scale (Table 1). The data set corrected with iMAR was also checked for the likelihood of newly developed artefacts.

Table 1 Scores for artefact and image quality analysis

Score	*Artefact*	*Image quality*
0	Very severe: very strong artefacts where anatomy is not visualized	Very poor
1	Severe: strong artefacts and limited evaluation of anatomical structures	Poor
2	Moderate: artefacts present but assessment of anatomical structures is not impaired	Fair
3	None or very mild	Good/excellent

Image quality

Image quality was defined as how precisely the CT images represented a maxillofacial pathology and was based on contrast, resolution and brightness perceived in the images while considering detection, verification and staging of a possible pathology. We also used a four-point rating scale for evaluation (Table 1).

Diagnostic utility

The capability of detecting hidden lesions or potential findings that were masked by the artefacts and identified or better detected after reconstruction with iMAR was considered as well as the diagnostic confidence in image interpretation.

Quantitative CT image analysis

To assess the effect of iMAR on the images of the areas without metal, Hounsfield units (HU) of two defined structures located above the metal region were measured and compared in the corrected and uncorrected data set. These structures were the right and left vitreous bodies and the right and left cerebellar hemispheres.

Statistics

For a pairwise comparison of corrected and uncorrected data set, the Wilcoxon signed-rank test was performed in SPSS® v. 23.0 (IBM Corp., New York, NY; formerly SPSS Inc., Chicago, IL) to determine statistical significance. A Wilcoxon test was applied to the rating criteria of the artefacts and image quality in the six defined regions. A p-value <0.05 was considered to be significant.

Results

Qualitative CT image analysis

Artefacts: The uncorrected data set exhibited extensive streaking artefacts that affected the assessment of the anatomical structures in regions R1, R2, L1 and L2 with limited pathology evaluation.

In the corrected data set, we noted a considerable reduction in the amount of artefacts (Figure 3). In the anterior regions, *i.e.* R1 and L1, the artefacts in the corrected data set were reduced by 2 points (from very severe to moderate artefacts) 20 times in the 34 regions of R1 and R2 (58.8%). The artefacts were reduced by 1 point 12 times (35.3%) (6 times from very severe to severe artefacts and 6 times from severe artefacts to moderate artefacts). In only two instances (5.9%), the artefacts did not significantly improve (once on the right and once on the left side).

In the middle regions (R2 and L2), the artefacts were reduced by 3 points (from very severe to none or very mild artefacts) twice (5.9%), by 2 points (7 times from very severe to moderate artefacts and 14 times from severe artefacts to none or very mild artefacts) 21 times (61.8%) and by 1 point (9 times from moderate to none

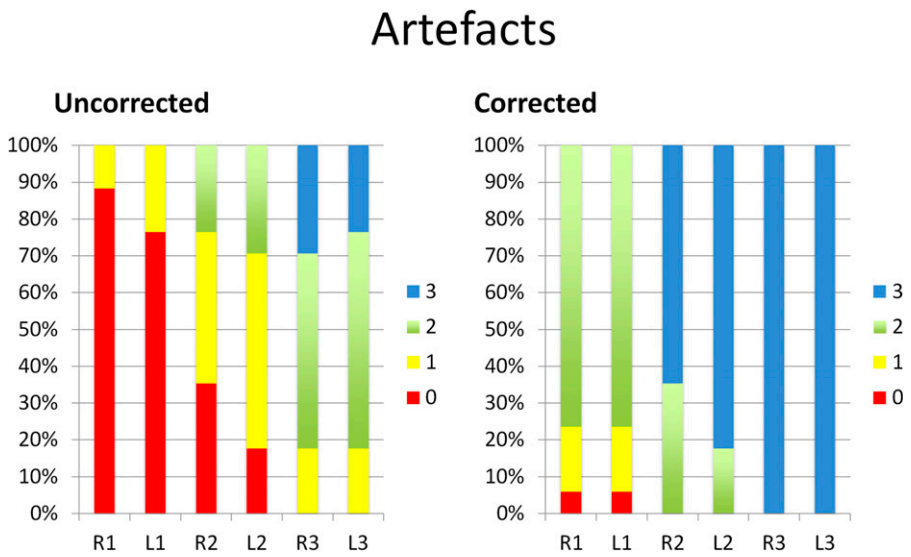

Figure 3 Artefact scores before (uncorrected) and after (corrected) application of iterative metal artefact reduction (iMAR) displayed on a 100% stacked column chart revealing score improvements due to artefact reduction using iMAR. The value 0 denotes a very poor condition; the value 3 denotes a good to excellent condition.

or very mild and twice from severe to moderate) 11 times (32.5%).

In the posterior regions (R3 and L3), the artefacts in the corrected data set were reduced by 2 points (from severe to none or very mild) 6 times (17.6%) and by 1 point (from moderate to none or very mild) 19 times (55.9%). The artefact score remained the same (none or very mild) seven times (20.6%).

With iMAR reconstruction, the artefact reduction in the six regions was statistically significant with a *p*-value of 0.000 for regions R1, L1, R2 and L2 and 0.001 for regions R3 and L3. Two examples of images from our study are shown in Figures 4 and 5.

For 4 (23.5%) of the 17 patients, blurring around the metal hardware in bone window was detected in the corrected images. This blurring was not observed in the uncorrected data set (Figure 7).

Image quality: The uncorrected data set was of poor quality, especially in the ventral and middle regions.

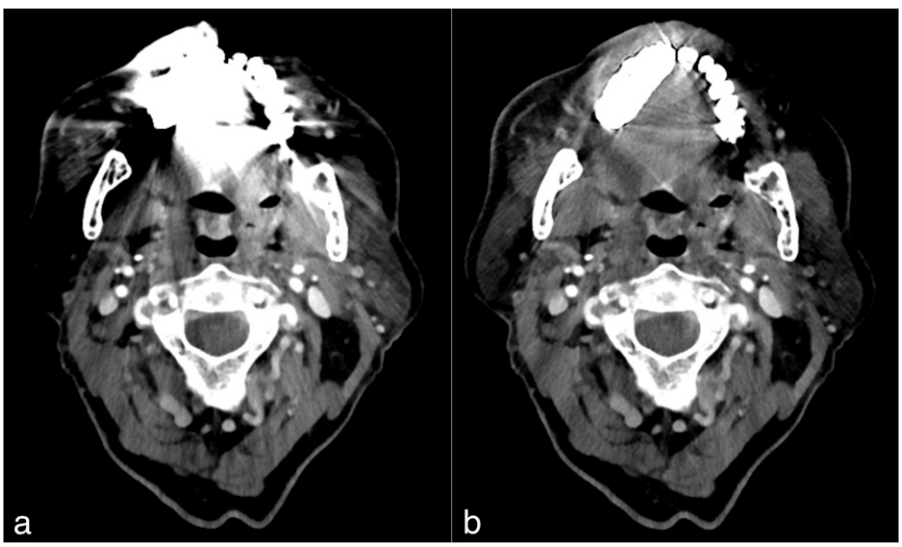

Figure 4 Images from the CT examination of a 72-year-old male after neck dissection and resection of a squamous cell carcinoma of the maxilla. CT slice at the level of the oropharynx before (a) and after (b) reconstruction with iterative metal artefact reduction (iMAR). The image before iMAR was severely distorted with artefacts owing to metal hardware in the maxilla, which affected the visualization of the anatomy, especially in the regions next to the metal implants. After the application of iMAR, a considerable reduction of artefacts and improvement in image quality was observed with visualization of the anatomy, especially next to the metal hardware. It can be noted that there is no change of quality in the regions less affected by artefacts, for example paraspinal regions.

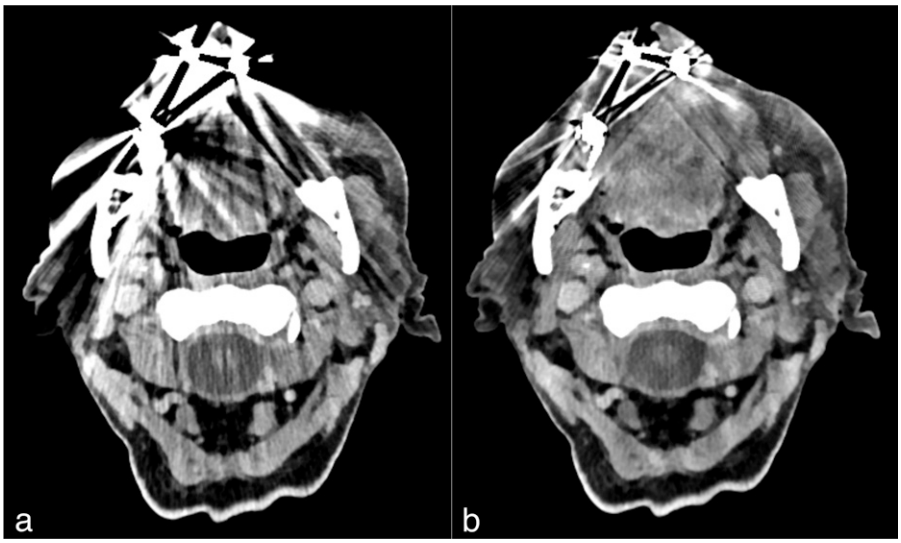

Figure 5 CT examination of an 81-year-old patient with chronic bisphosphonate-induced osteonecrosis. CT slice at the level of the oropharynx before (a) and after (b) post-processing with iterative metal artefact reduction (iMAR). Several artefacts were present near the implanted metal hardware in the maxilla before post-processing and were considerably reduced after the application of iMAR, which improved the quality of the image.

In the corrected data set, image quality was improved (Figure 6). Image quality in the anterior regions (R1 and L1) was improved by 2 points (from very poor to fair, 7 times on the right side and 8 times on the left side) 15 times (44.1%) and by 1 point (12 times from very poor to poor, 6 times from poor to fair and once from fair to good/excellent) 19 times (55.9%).

In the middle regions (R2 and L2), image quality improved by 3 points (from very poor to good/excellent) twice (5.9%), by 2 points (7 times, very poor to fair and 14 times from poor to good/excellent) 21 times (61.8%) and by 1 point (8 times from fair to good/excellent and once from poor to fair) 9 times (26.5%). In two instances (5.9%), the image quality did not change (good/excellent).

In the posterior regions (R3 and L3), the image quality improved by 2 points (from poor to good/excellent) 6 times (26.5%) and by 1 point (from fair to good/excellent) 18 times (52.9%). In 10 instances (29.4%), the quality remained the same (good/excellent). Two examples with improvement of image quality from our study are shown in Figures 4 and 5.

With iMAR reconstruction, the improvement in image quality in the six regions was statistically significant, with a *p*-value of 0.000 for regions R1, L1, R2 and L2 and 0.001 for regions R3 and L3.

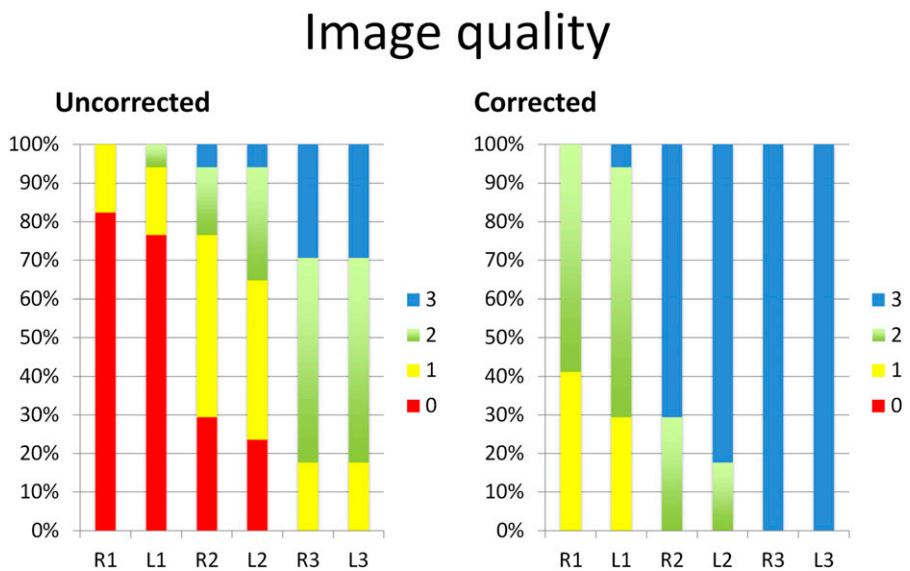

Figure 6 Image quality scores before (uncorrected) and after (corrected) application of iterative metal artefact reduction (iMAR) displayed on a 100% stacked column chart revealing quality improvement of images after post-processing with iMAR.

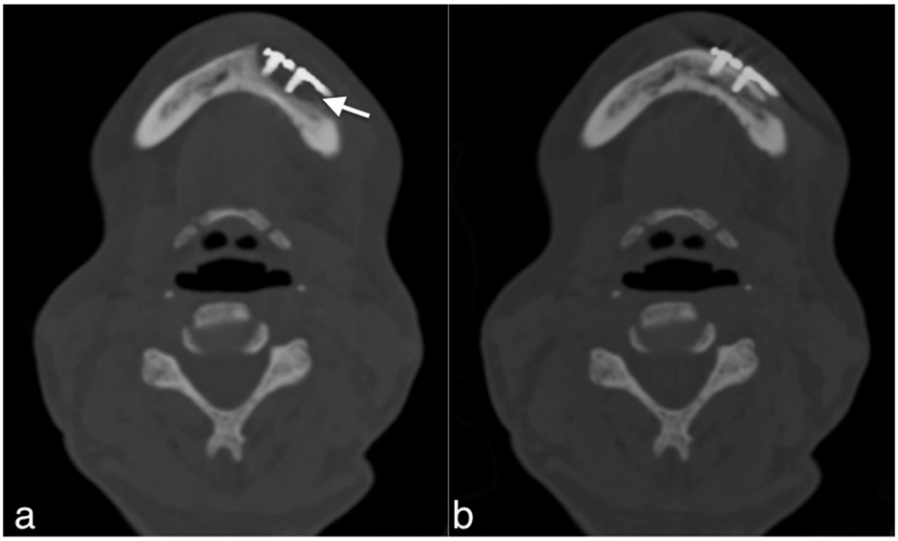

Figure 7 CT examination of a 58-year-old patient who was treated by osteosynthesis of the mandible following pathological fracture due to osteonecrosis: the corrected images with iterative metal artefact reduction (a) are showing an osteolysis-like area around the screws (arrow). Such artefacts were found in a small number of patients. Misinterpretation was avoided by comparing the corrected data set with the uncorrected data set (b).

Diagnostic utility: In 10 and 11 of the 17 patients (58.8% and 64.7% patients), new findings in the corrected data set were noted in the soft tissue and in the bone window, respectively. These findings could not be evaluated during the standard reconstruction without iMAR because they were masked by artefacts. Findings included (a) focal hyperostosis around the implanted osteosynthesis screws (two patients); (b) dental decay of the mandibular central incisors due to piercings in the oral cavity (one patient); (c) lamellar periosteal reaction at the alveolar ridge (one patient); (d) reactive hyperostosis in the lingual cortex of the mandibular ramus (one patient); and (e) better visualization and evaluation of the screws of the osteosynthesis of the pins of implanted tooth and bone cement (six patients).

Regarding the soft-tissue window, the following findings were noted after post-processing with iMAR: (a) hypertrophy of the pharyngeal and palatine tonsils with tinny calcifications in two patients; (b) asymmetry of the muscles of mastication (buccinators/masseter) in two patients; (c) reactive swelling of the Waldeyer's ring and lymph nodes in the parapharyngeal space in the context of throat infection (three patients); (d) a simple cyst in the palatine tonsil (one patient); and (e) fatty atrophy of the tongue (one patient) and better delineation of a subcutaneous haematoma after trauma of the right maxillary sinus (one patient). In image evaluation, both examiners reported greater confidence in the iMAR-corrected images than in the original images.

Quantitative CT image analysis

HU measurements for neither the vitreous body nor the cerebellum revealed any significant differences between the uncorrected and corrected data sets (Table 2).

Discussion

In this study, we evaluated the recently introduced artefact reduction algorithm "iMAR". iMAR was utilized during the routine workflow for patients with metal hardware in the maxillofacial region who had postoperative CT examinations. These patients were undergoing complex reconstructive maxillofacial surgery and presented with metal implants in the oral cavity. The patients underwent imaging for various clinical reasons such as trauma, infection, stroke or postoperative follow-up.

iMAR is an add-on tool that can be applied to images after scanning the patient. iMAR does not change the CT scan parameters, and no additional scans are required. The radiation dose also remains the same. From the operator perspective, utilizing iMAR is similar to the standard SAFIRE, which is very simple and does not require additional training.

The iMAR algorithm significantly reduced artefacts and improved image quality. The extent of artefact reduction is related to the volume and type of metal, as well as the distance of the tissue from the metal implants. The effect of iMAR was particularly noticeable in the regions most affected by artefacts, such those that abut or are near to maxillofacial implants, namely the oral cavity, submandibular space, pharyngeal mucosal space, masticator space, parotid space and retropharyngeal space. Complete removal of artefacts in regions adjacent to metal turned out to be not possible in every patient.

Artefacts in the perivertebral and posterior cervical spaces were also reduced, and image quality increased. In addition, the diagnostic value of the CT scans after iMAR increased owing to the ability of detecting

Table 2 Comparison of Hounsfield units measured in areas, which were not affected by artefacts, before (uncorrected) and after (corrected) iterative metal artefact reduction application

Number	*Data set*	*Right vitreous body*	*Left vitreous body*	*Right cerebellum*	*Left cerebellum*
P1	Uncorrected	11	12	51	45
	Corrected	11	12	51	45
P2	Uncorrected	30	37	35	44
	Corrected	30	37	34	44
P3	Uncorrected	30	26	36	35
	Corrected	30	26	35	35
P4	Uncorrected	34	29	40	44
	Corrected	35	29	40	44
P5	Uncorrected	25	41	42	47
	Corrected	25	40	41	47
P6	Uncorrected	23	34	39	42
	Corrected	23	35	39	41
P7	Uncorrected	36	40	42	41
	Corrected	36	40	42	41
P8	Uncorrected	36	34	47	55
	Corrected	36	34	46	54
P9	Uncorrected	40	36	27	33
	Corrected	40	36	27	33
P10	Uncorrected	22	20	55	54
	Corrected	21	20	55	53
P11	Uncorrected	30	34	34	36
	Corrected	31	35	34	36
P12	Uncorrected	35	28	36	37
	Corrected	35	28	36	35
P13	Uncorrected	15	12	59	55
	Corrected	15	12	57	54
P14	Uncorrected	27	27	45	40
	Corrected	27	25	44	39
P15	Uncorrected	40	43	43	39
	Corrected	40	43	43	37
P16	Uncorrected	41	40	34	32
	Corrected	42	39	31	32
P17	Uncorrected	33	30	31	40
	Corrected	32	29	28	36

findings that were masked by artefacts. There was no change in the quality in regions distant from metal implants.

Previous studies evaluated the usefulness of iMAR and its prototypes in reducing metal artefacts. These reports focused on hip arthroplasties,[5,10,14–18] shoulder arthroplasties,[13] internal fixation hardware,[12] dental hardware[14,19] and spinal hardware.[20,21] Our findings are consistent with those of previous studies. Furthermore, our findings demonstrate the utility of using iMAR in the post-operative phase and show that additional findings can be discovered after artefact reduction. We also found that new artefacts can appear after applying iMAR, as observed in a few of our patients. In these patients, we observed blurring around the metal hardware in the bone window, which had the potential to be misinterpreted as osteolysis. This blurring probably resulted from data loss near the metal edge, which could not be recovered during the interpolation process. This type of artefact was noted with one of the prototypes of iMAR[8] but is substantially reduced in the current version of iMAR as a result of the multiple iterations before producing the final image.[13] The presence of these artefacts is the reason why some institutes do not utilize iMAR, or in-painting algorithms, in their clinical routine.[22] In our patients, such misinterpretation could be avoided by comparing the corrected and uncorrected data sets. Thus, detecting osteolysis-like lesions with iMAR requires careful comparison with the source images. The added diagnostic value of iMAR, as described previously, far outweighs this disadvantage and should not be ignored. Further research focusing on the diagnostic accuracy of iMAR for osseous lesions is required.

In our experience, iMAR is valuable for the detection of soft-tissue pathologies located next to the metal hardware but is masked by metal artefacts in the standard reconstruction. In our institution, iMAR is routinely used not only for patients with metal implants in the maxillofacial region but also for those with ventriculoperitoneal shunts, clipping and coiling of intracerebral aneurysms, reimplantation of skull bones after osteoclastic craniotomy or after spinal fusion surgery. In all of these cases, the iMAR-corrected and iMAR-uncorrected data sets are compared to ensure that no information is lost.

Limitations

This was a retrospective study with a small cohort of patients and a heterogeneous sample. The study was performed using iMAR (Siemens Healthcare). Thus, the results do not necessarily apply to similar algorithms from other vendors. Our analysis focused on the level of the oropharynx, which in most cases presents with the maximum degree of artefacts. Obtaining accurate HU for a quantitative analysis at the level of the artefacts was challenging because there were no constant values to compare the HU after post-processing with iMAR (the HU values in the original uncorrected data are already corrupted). Thus, a quantitative analysis was performed only outside the artefact regions.

Assessing the effect of different scanning parameters with iMAR on image quality was beyond the scope of this study but could represent an important consideration in developing a method to reduce the radiation dose while maintaining image quality.

Conclusions

iMAR is a powerful tool for reducing artefacts resulting from maxillofacial metal hardware. iMAR significantly improves image quality and enhances the evaluation of adjacent soft-tissue structures. iMAR also increases the observer confidence in detecting pathologies.

Acknowledgments

We thank the CT team and their leader Mrs Nadja Feusi for their contribution to this study by post-processing the images with iMAR.

References

1. Boas FE, Fleischmann D. CT artifacts: causes and reduction techniques. *Imaging Med* 2012; **4**: 229–40. http://www.edboas.com/science/CT/0012.pdf
2. De Man B, Nuyts J, Dupont P, Marchal G, Suetens P. Metal streak artifacts in X-ray computed tomography: a simulation study. *IEEE Trans Nucl Sci* 1999; **46**: 691–6. doi: https://doi.org/10.1109/23.775600
3. Meinel FG, Bischoff B, Zhang Q, Bamberg F, Reiser MF, Johnson TR. Metal artifact reduction by dual-energy computed tomography using energetic extrapolation: a systematically optimized protocol. *Invest Radiol* 2012; **47**: 406–14. doi: https://doi.org/10.1097/RLI.0b013e31824c86a3
4. Lell MM, Meyer E, Kuefner MA, May MS, Raupach R, Uder M, et al. Normalized metal artifact reduction in head and neck computed tomography. *Invest Radiol* 2012; **47**: 415–21. doi: https://doi.org/10.1097/RLI.0b013e3182532f17
5. Subhas N, Polster JM, Obuchowski NA, Primak AN, Dong FF, Herts BR, et al. Imaging of arthroplasties: improved image quality and lesion detection with iterative metal artifact reduction, a new CT metal artifact reduction technique. *AJR Am J Roentgenol* 2016; **207**: 378–85. doi: https://doi.org/10.2214/AJR.15.15850
6. Axente MM, Paidi AA, von Eyben RR, Zeng CC, Bani-Hashemi AA, Krauss A, et al. Clinical evaluation of the iterative metal artifact reduction algorithm for CT simulation in radiotherapy. *Med Phys* 2015; **42**: 1170–83. doi: https://doi.org/10.1118/1.4906245
7. Meyer E, Raupach R, Lell M, Schmidt B, Kachelriess M. Normalized metal artifact reduction (NMAR) in computed tomography. *Med Phys* 2010; **37**: 5482–93. doi: https://doi.org/10.1118/1.3484090
8. Meyer E, Raupach R, Lell M, Schmidt B, Kachelrieß M. Frequency split metal artifact reduction (FSMAR) in computed tomography. *Med Phys* 2012; **39**: 1904–16. doi: https://doi.org/10.1118/1.3691902
9. Wuest W, May MS, Brand M, Bayerl N, Krauss A, Uder M, et al. Improved image quality in head and neck CT using a 3D iterative approach to reduce metal artifact. *AJNR Am J Neuroradiol* 2015; **36**: 1988–93. doi: https://doi.org/10.3174/ajnr.A4386
10. Morsbach F, Bickelhaupt S, Wanner GA, Krauss A, Schmidt B, Alkadhi H, et al. Reduction of metal artifacts from hip prostheses on CT images of the pelvis: value of iterative reconstructions. *Radiology* 2013; **268**: 237–44. https://doi.org/10.1148/radiol.13122089
11. Morsbach F, Wurnig M, Kunz DM, Krauss A, Schmidt B, Kollias SS, et al. Metal artefact reduction from dental hardware in carotid CT angiography using iterative reconstructions. *Eur Radiol* 2013; **23**: 2687–94. doi: https://doi.org/10.1007/s00330-013-2885-z
12. Winklhofer S, Benninger E, Spross C, Morsbach F, Rahm S, Ross S, et al. CT metal artefact reduction for internal fixation of the proximal humerus: value of mono-energetic extrapolation from dual-energy and iterative reconstructions. *Clin Radiol* 2014; **69**: e199–206. doi: https://doi.org/10.1016/j.crad.2013.12.011
13. Subhas N, Primak AN, Obuchowski NA, Gupta A, Polster JM, Krauss A, et al. Iterative metal artifact reduction: evaluation and optimization of technique. *Skeletal Radiol* 2014; **43**: 1729–35. doi: https://doi.org/10.1007/s00256-014-1987-2
14. Bongers MN, Schabel C, Thomas C, Raupach R, Notohamiprodjo M, Nikolaou K, et al. Comparison and combination of dual-energy- and iterative-based metal artefact reduction on hip prosthesis and dental implants. *PLoS One* 2015; **10**: e0143584. doi: https://doi.org/10.1371/journal.pone.0143584
15. Andersson KM, Nowik P, Persliden J, Thunberg P, Norrman E. Metal artefact reduction in CT imaging of hip prostheses—an evaluation of commercial techniques provided by four vendors. *Br J Radiol* 2015; **88**: 20140473. doi: https://doi.org/10.1259/bjr.20140473
16. Higashigaito K, Angst F, Runge VM, Alkadhi H, Donati OF. Metal artifact reduction in pelvic computed tomography with hip prostheses: comparison of virtual monoenergetic extrapolations from dual-energy computed tomography and an iterative metal artifact reduction algorithm in a phantom study. *Invest Radiol* 2015; **50**: 828–34. doi: https://doi.org/10.1097/RLI.0000000000000191
17. Abdoli M, Mehranian A, Ailianou A, Becker M, Zaidi H. Assessment of metal artifact reduction methods in pelvic CT. *Med Phys* 2016; **43**: 1588–97. doi: https://doi.org/10.1118/1.4942810
18. Boos J, Sawicki LM, Lanzman RS, Thomas C, Aissa J, Schleich C, et al. Metal artifact reduction (MAR) based on two-compartment physical modeling: evaluation in patients with hip implants. *Acta Radiol* 2016; **58**: 70–76. https://doi.org/10.1177/0284185116633911
19. Weiß J, Schabel C, Bongers M, Raupach R, Clasen S, Notohamiprodjo M, et al. Impact of iterative metal artifact reduction on diagnostic image quality in patients with dental hardware. *Acta Radiol* 2016. [Epub ahead of print]. https://doi.org/10.1177/0284185116646144
20. Kaewlek T, Koolpiruck D, Thongvigitmanee S, Mongkolsuk M, Thammakittiphan S, Tritrakarn S, et al. Metal artifact reduction and image quality evaluation of lumbar spine CT images using metal sinogram segmentation. *J Xray Sci Technol* 2016; **23**: 649–66. doi: https://doi.org/10.3233/XST-150518
21. Kotsenas AL, Michalak GJ, DeLone DR, Diehn FE, Grant K, Halaweish AF, et al. CT metal artifact reduction in the spine: can an iterative reconstruction technique improve visualization? *AJNR Am J Neuroradiol* 2015; **36**: 2184–90. doi: https://doi.org/10.3174/ajnr.A4416
22. Sutter R, Dietrich T. Reduktion von metallartefakten in der muskuloskelettalen bildgebung. Radiologie 2016; **16**: 127–144. doi: https://doi.org/10.1055/s-0042-105421